60315 POIKILITIC IMPACT MELT 787 g

INTRODUCTION: 60315 is a greenish-gray, very coherent poikilitic impact melt (Fig. 1) that is enriched in incompatible elements compared with most other Apollo 16 rocks. Its texture and major element chemistry is typical of Apollo 16 poikilitic rocks. Macroscopically the silicate phases are homogeneously distributed but the grain size is somewhat variable. The sample was collected 5 m north of the Lunar Module, where it was only slightly buried. Its orientation is known, and the exposed lunar surface has many zap pits, with few on other surfaces.


FIGURE 1. Scale in cm. S-72-41572B.

PETROLOGY: Bence et al. (1973), Simonds et al. (1973), Hodges and Kushiro (1973) and Walker et al (1973) provide detailed petrographic descriptions of 60315. All note the anhedral orthopyroxene ($Wo_4En_{80}$) oikocrysts up to 3 mm long which enclose abundant

laths and clasts of plagioclase, rare olivines ($Fo_{74-77}$) and opaques (Fig. 2). Plagioclase clasts often have very calcic cores ($An_{95-97}$) and narrow, more sodic rims (down to $An_{89}$). Augite, olivine, ilmenite and armalcolite discontinuously rim some oikocrysts. Simonds et al. (1973) give a mode of 55% plagioclase + mesostasis, 34% orthopyroxene, 4% augite, 1% olivine and 1% opaques. Mineral compositions are shown in Figure 3. Similar data are presented by Vaniman and Papike (1981).

Areas interstitial to the oikocrysts have textures ranging from granular to subophitic and account for ~10% of the rock. Most of the interstices are enriched in K, Na, Si, S, P and opaque minerals. Rounded vesicles are common. Bence et al. (1973) report one interstitial region with euhedral plagioclase crystals in a troilite matrix. In many places the oikocrysts grade into a fine-grained clastic matrix of plagioclase ($An_{71-80}$), olivine ($Fo_{71-80}$), pyroxene, opaques and lithic fragments. Plagioclase grains often show textural signs of re-equilibration with the matrix. The small (~0.5 mm) subophitic patches consist of interlocking plagioclase laths ($An_{90-95}$) with interstitial olivine ($Fo_{71-73}$), zoned augite ($Wo_{35-41}Ens_{53-48}$), orthopyroxene ($Wo_3En_{82}$) and minor K-feldspar, ilmenite, armalcolite, phosphates, silica, metal and troilite.

Hewins and Goldstein (1975b), Ridley and Adams (1976) and Hodges and Kushiro (1973) calculated equilibration temperatures based on pyroxene, olivine and metal phase geothermometers. The silicate phases equilibrated at ~1000-1200°C whereas the metallic phases record a temperature of ~600°C. Metal compositions (Fig. 4) are given by L. Taylor et al. (1973a), Reed and Taylor (1974) and Misra and Taylor (1975). Meyer (1979) determined trace elements in plagioclase in 60315 using the ion microprobe.

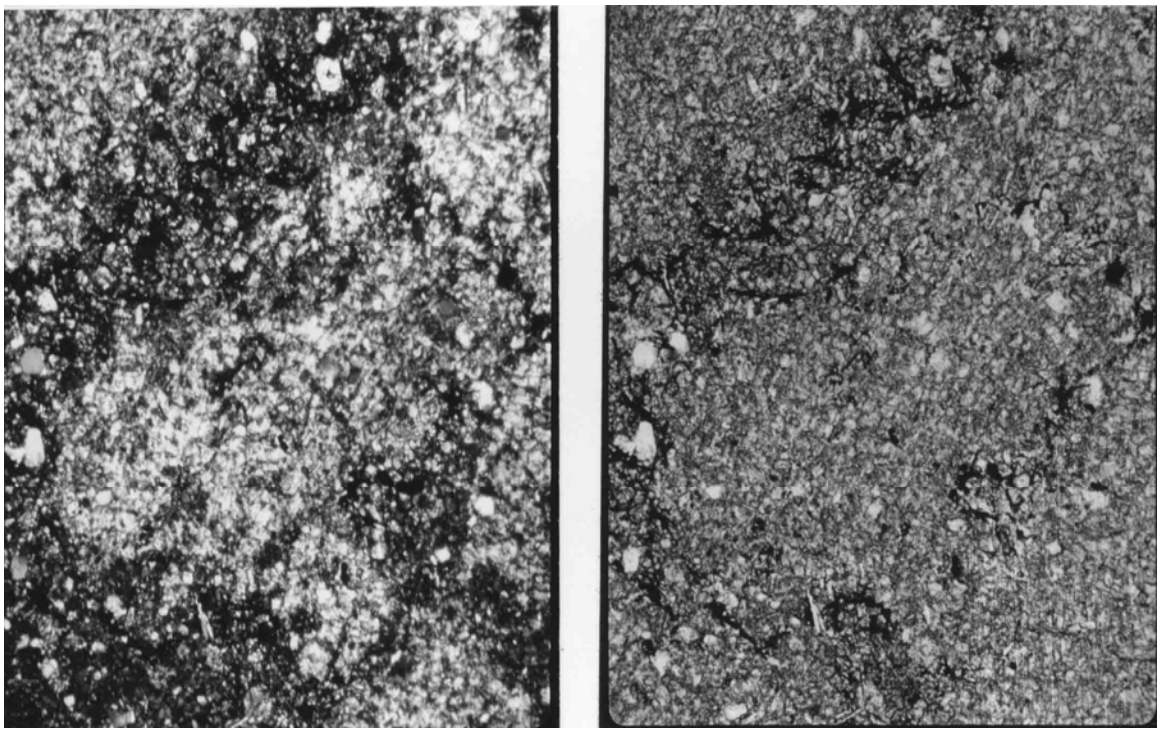

FIGURE 2. 60315,15. Same view, width 2 mm. a) xpl, b) ppl.

EXPERIMENTAL PETROLOGY: Ford et al. (1974) experimentally determined the phase relations of 60315. Spinel is the equilibrium liquidus phase (1300°C) followed by olivine (1276°) and plagioclase (1256°). Pyroxene was not produced even at their lowest temperature (1200°). This is consistent with textural evidence which indicates that olivine and plagioclase preceded pyroxene.

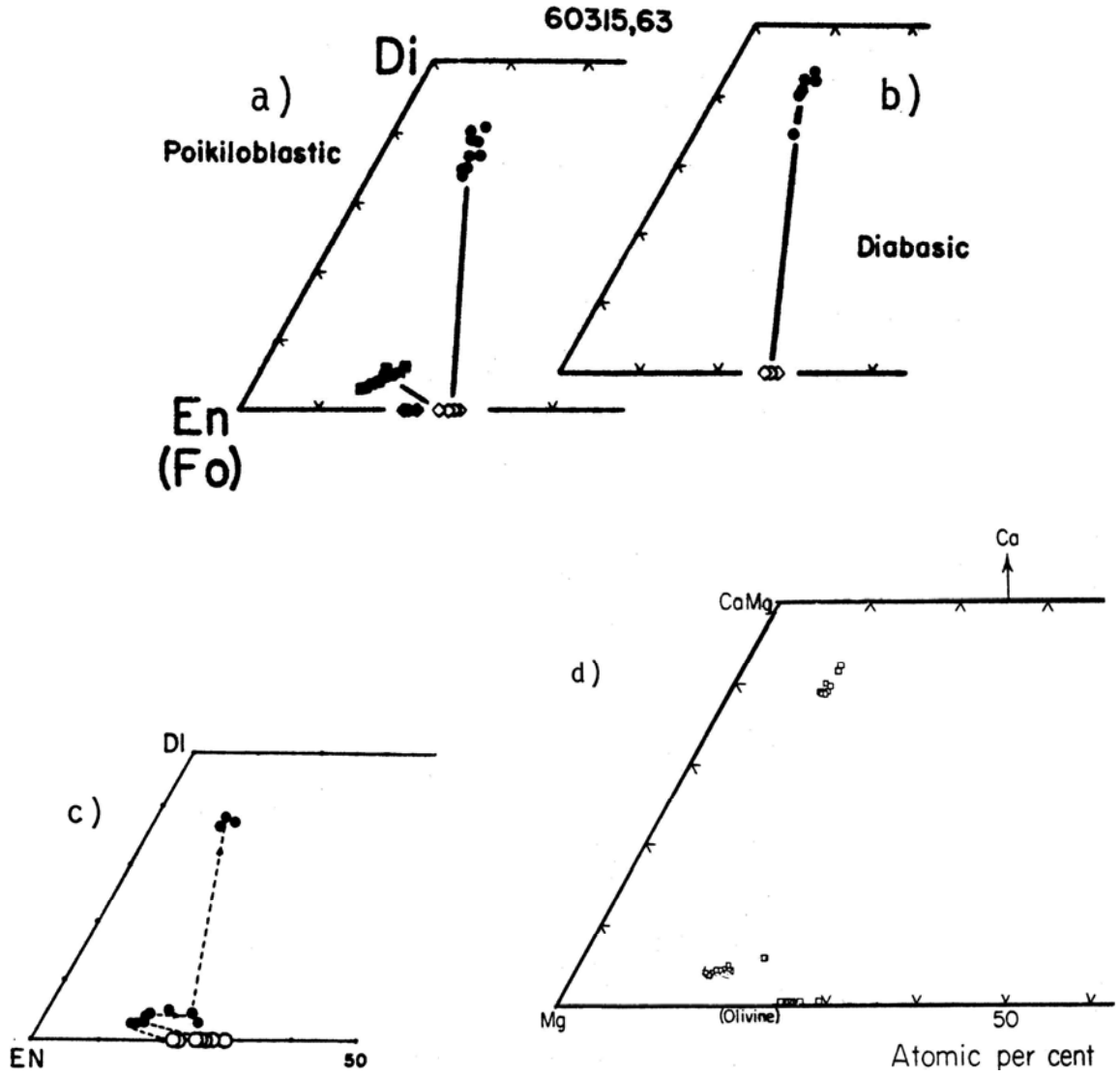


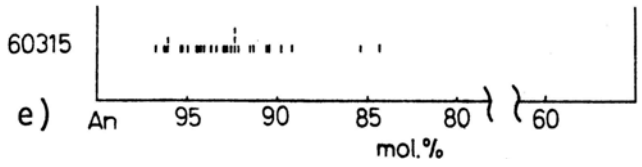

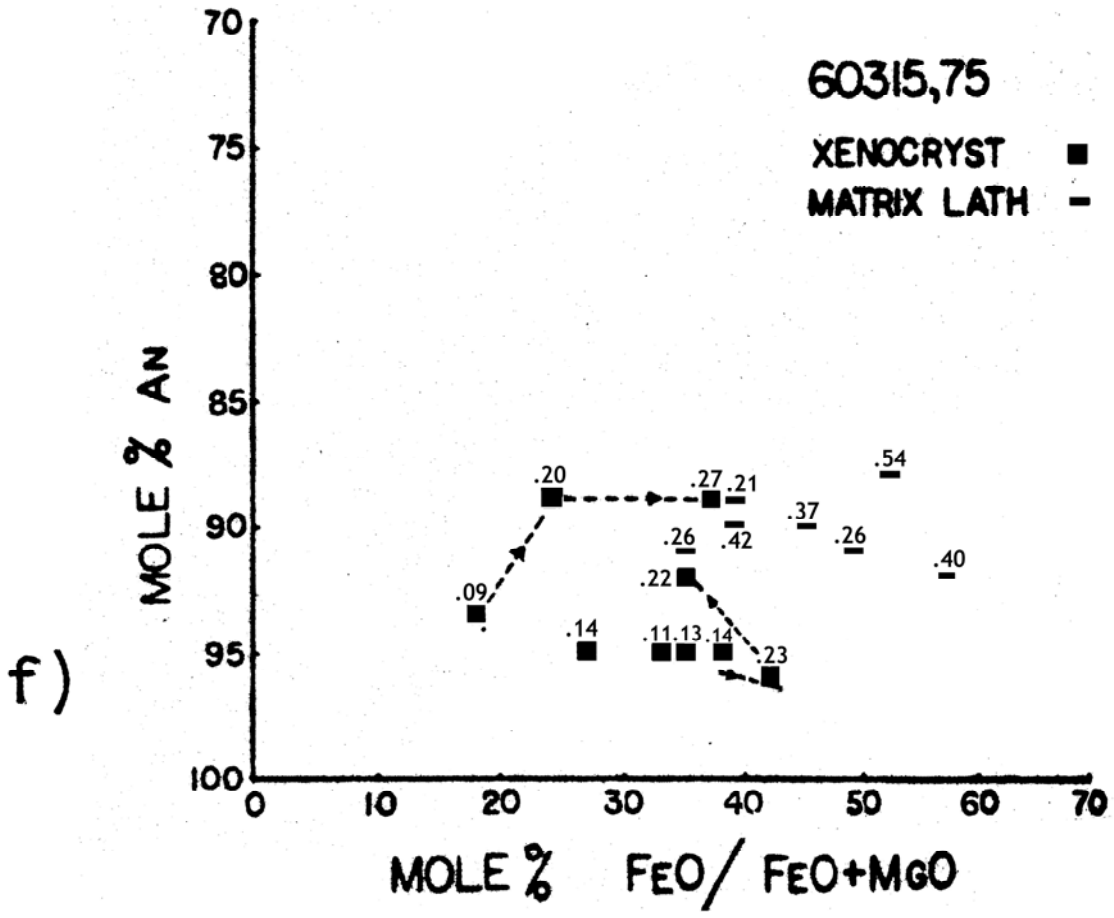


FIGURE 3. Compositions of pyroxenes, olivines, and plagioclases in 60315.
a) and b) Bence et al. (1973).
c) Walker et al. (1973).
d) and e) Hodges and Kushiro (1973).
f) Walker et al. (1973).

CHEMISTRY: Chemical studies of 60315 are listed in Table l and a summary chemistry in Table 2. Rare earth element abundances and patterns are shown in Figure 5.

The major element chemistry of 60315 is very similar to Apollo 15 "Fra Mauro basalt" glasses, and it lies very near the olivine-plagioclase cotectic of the OL-AN-SI system (Fig. 6). Rare earth element abundances are among the highest measured in any Apollo 16 sample (see also 62235 and 65015) and have a KREEP pattern (Table 3 and Fig. 5). 60315 is not simply remelted local soil: it is much lower in $A1_2O_3$ and higher in rare earth elements. Siderophile abundances vary from split to split (e.g. reported Ni values range from 191-1400 ppm) but all indicate substantial amounts of meteoritic material.

Hertogen et al. (1977) considered the anomalously low Ir/Au ratio indicative of a distinct meteoritic component and assigned 60315 to a new meteoritic signature, Group ILL. Volatiles also vary by two orders of magnitude between different splits (e.g. reported Zn ranges from 0.3-12 ppm).

Sato (1976) measured the oxygen fugacity of 60315 directly using the solid-electrolyte oxygen cell method. Fugacity values at a series of temperatures are given in Table 3. Hash and Haselton (1975) calculated the equilibrium silica activity of a melt with the composition of 60315. They conclude that Apollo 16 crystalline rocks 60315 and 68416 have higher initial silica activities than Apollo 17 high-Ti mare basalts.

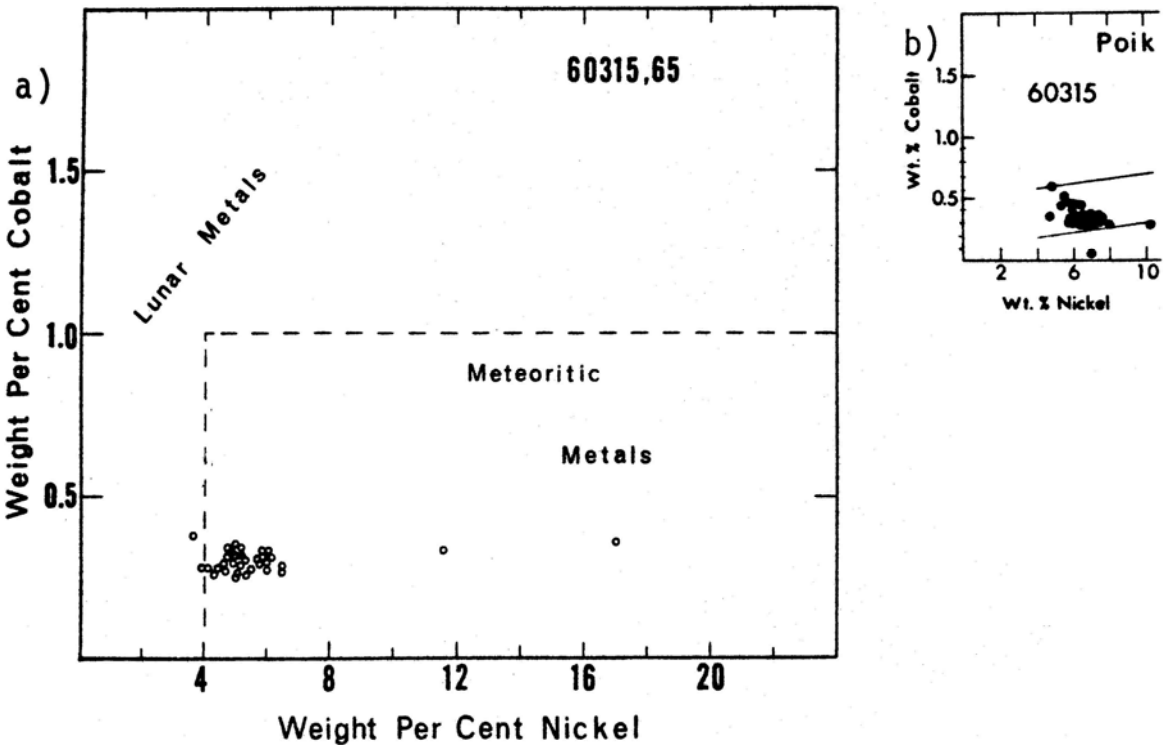


FIGURE 4. Metal compositions;
a) from L. Taylor et al.(1973a). b) from Misra and Taylor (1975).

GEOCHRONOLOGY AND RADIOGENIC ISOTOPES: Whole rock Rb-Sr data are presented by Nyquist et al. (1973). Model ages of $T_{BABI}$ = 4.41 ± 0.06 b.y. and $T_{LUNI}$ = 4.44 ± 0.06 b.y. were calculated. KRFEP-rich rocks 60315, 62235, and 65015 define a whole rock Rb-Sr isochron of 4.42 ± 0.38 b.y. with initial $^{87}Sr/^{86}Sr$: 0.6992 ± 9. Assuming a 3.9 b.y. age for these rocks yields an initial $^{87}Sr/^{86}Sr$ = 0.70040 ± 15 (Nyquist et al., 1973).

Well defined $^{39}Ar$-$^{40}Ar$ plateau ages of 4.03 ± 0.03, 3.94 ± 0.05 and 3.91 ± 0.02 b.y. were obtained by Kirsten et al. (1973), Husain and Schaeffer (1973) and Schaeffer et al. (1976) respectively (Fig. 7). Schaeffer et al. (1976) also report a K-Ar age of 3.69 ± 0.01 b.y.

TABLE 1. Chemical studies of 60315.

| Reference | Split # | Elements analyzed |
|---|---|---|
| Rose et al. (1973) | ,88 | majors, trace, incl. some REEs |
| Hubbard et al. (1973) | ,3 | majors, REEs, other trace |
| Hubbard et al. (1973) | ,57 | majors |
| Morrison et al. (1973) | ,53 | majors, REEs, other trace |
| LSPET (1973) | ,3 | majors, trace |
| S.R. Taylor et al. (1973) | ,58 | majors, REEs, other trace |
| Laul et al. (1974) | ,157 | majors, REEs, other trace |
| Wänke et al. (1976) | ,87; ,103 | majors, REEs, other trace |
| Wänke et al. (1977) | ,87 | V |
| Nyquist et al. (1973) | ,3 | Rb, Sr |
| Kirsten et al. (1973) | ,19 | K, Ca |
| Nunes et al. (1973) | ,81 | U, Th, Pb |
| Nunes (1975) | ,81 ? | U, Th, Pb |
| Eldridge et al. (1973) | ,0 | U, Th, K |
| Moore et al. (1973) | ,4 | C |
| Ganapathy et al. (1974) | ,79 | meteoritic sids. and vols. |
| Flory et al. (1973) | ,52 | volatile organogenic compounds |

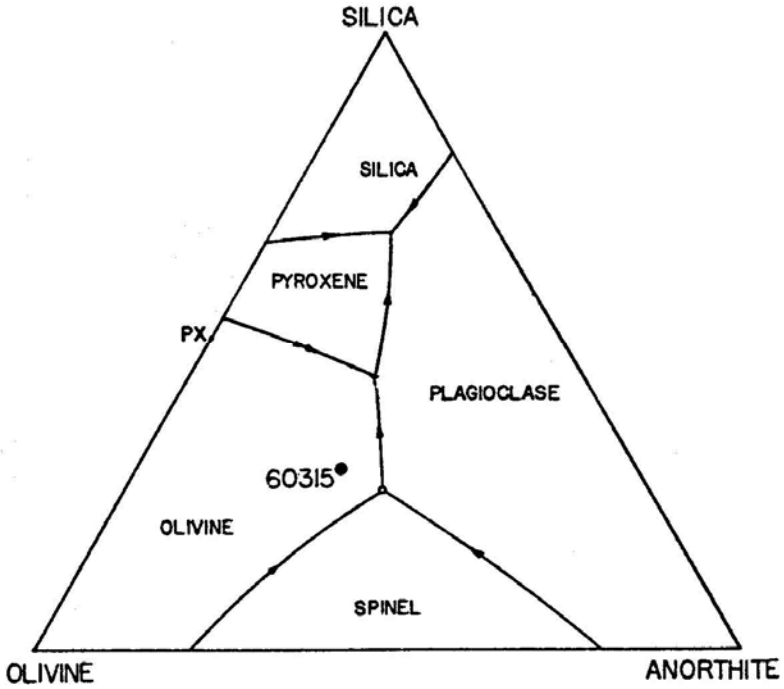


FIGURE 5. From Walker et al. (1973).

TABLE 2. Summary chemistry of 60315.

| | |
|---|---|
| $SiO_2$ | 46.5 |
| $TiO_2$ | 1.31 |
| $Al_2O_3$ | 17.2 |
| $Cr_2O_3$ | 0.21 |
| FeO | 9.3 |
| MnO | 0.11 |
| MgO | 13.2 |
| CaO | 10.2 |
| $Na_2O$ | 0.61 |
| $K_2O$ | 0.40 |
| $P_2O_5$ | 0.48 |
| Sr | 155 |
| La | 49 |
| Lu | 2.1 |
| Rb | 9.7 |
| Sc | 15 |
| Ni | ~800 |
| Co | ~50 |
| Ir ppb | ~10 |
| Au ppb | ~17 |
| C | ~20 (?) |
| N | ~20 |
| S | 1300 |
| Zn | ~5 (?) |
| Cu | 11 |

Oxides in wt%; others in ppm except as noted.

TABLE 3. Oxygen Fugacity of 60315.

| T (°C) | -log $fo_2$ (atm) |
|---|---|
| 1000 | 16.2 |
| 1050 | 15.4 |
| 1100 | 14.6 |
| 1150 | 13.9 |
| 1200 | 13.2 |

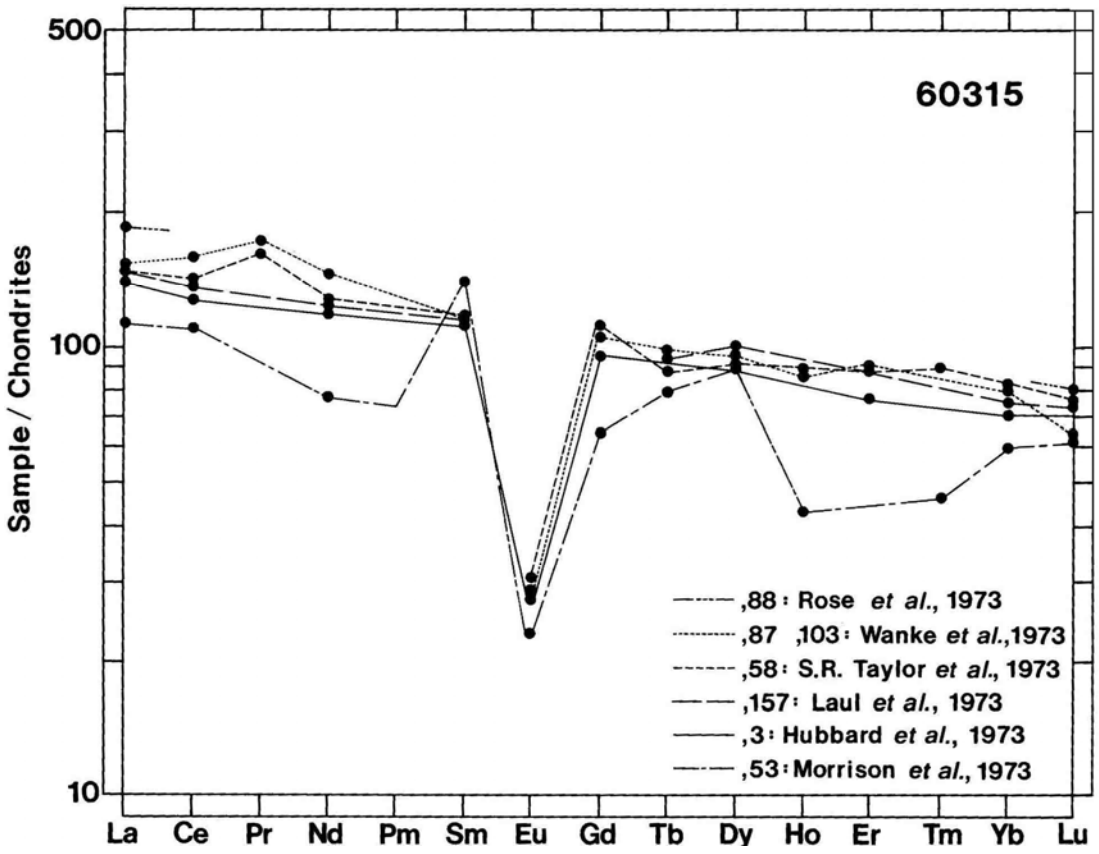


FIGURE 6. Rare earths.

Nunes et al. (1973) and Nunes (1975) report U-Th-Pb data. 60315 is very enriched in in-situ radiogenic lead ($^{206}$Pb/204Pb, >10,000). Nearly all of the original lead was probably expelled during a period of intense heating. A Pb-Pb internal isochron yields an age of 3.99 ± 0.01 b.y. (Fig. 8). The bulk rock is concordant at 3.93 b.y. (Nunes, 1975) rather than slightly discordant at 3.99 b.y. as originally reported by Nunes et al. (1973).

RARE GAS/EXPOSURE AGE: Kirsten et al. (1973) report a $^{38}$Ar age of 4.5 ± 1 m.y. Schaeffer et al. (1976) determined a maximum $^{38}$Ar age of 11 m.y. with a more probable age of 5 ± 3 m.y. Keith and Clark (1974) calculate a $^{26}$Al maximum exposure age of 2.3 m.y. Eldridge et al. (1973) provide abundance data on cosmogenic radionuclides determined by γ-ray spectroscopy and Keith et al. (1975) discuss the saturated activities of specific short-lived, cosmogenic radionuclides.

MICROCRATERS AND TRACKS: Neukum et al. (1973), Fechtig et al. (1974) and Nagel et al. (1975) provide data on microcraters on 60315. The rock has had a simple exposure history and the surfaces are in production. Nagel et al. (1975) report small metallic spherules enriched in Fe, Ni and S suspended within some of the crater glass linings.

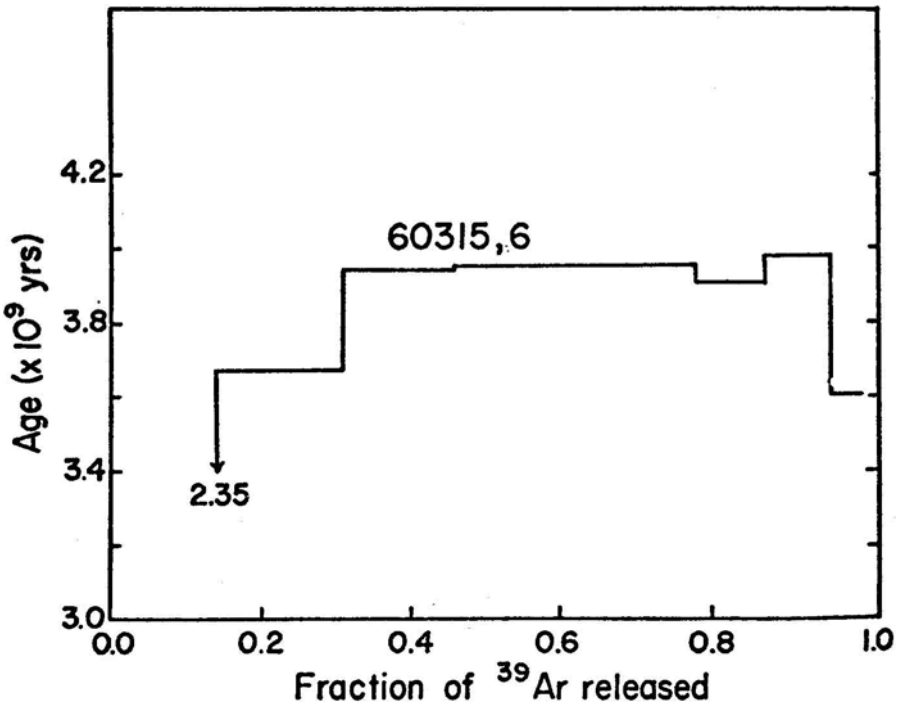


FIGURE 7a. Ar release; from Husain and Shaeffer (1973)

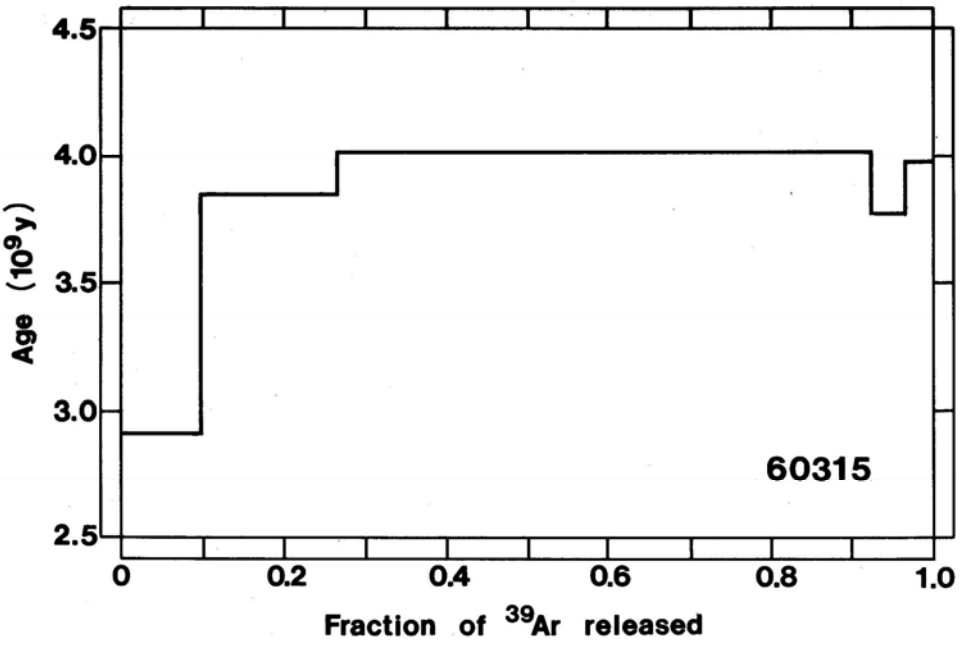


FIGURE 7b. Ar release; from Kirsten et al. (1973).

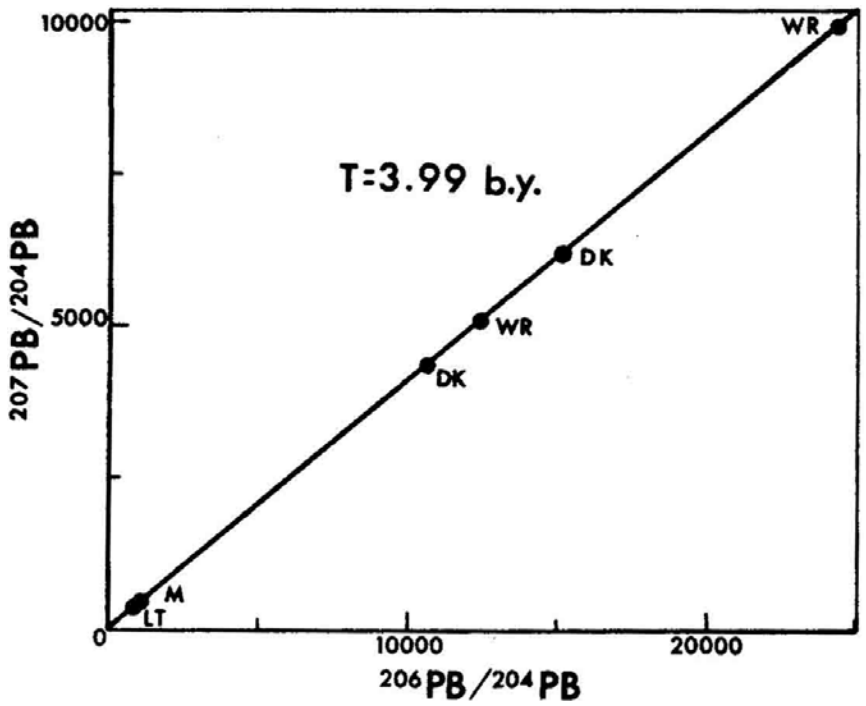


FIGURE 8. Pb-Pb isochron; from Nunes et al. (1973).

PHYSICAL PROPERTIES: Brecher et al. (1973), Nagata et al. (1973) and Schwerer and Nagata (1976) provide magnetic data and discussion (Figs. 9 and 10). Coarse multidomain grains predominate over a superparamagnetic fraction. About 40% of the metallic iron component in this rock is kamacite with ~5% Ni. A very small component of NRM and IRM is stable against AF-demagnetization (Fig. 10). Measured magnetic parameters of 60315 vary from chip to chip by over an order of magnitude (see e.g. Brecher et al., 1973) possibly relating to the inhomogeneous distribution of metallic phases.

Mossbauer analyses are given by Brecher et al. (1973), Huffman et al. (1974) and Huffman and Dunmyre (1975) (Fig. 11). Tsay and Bauman (1977) studied paramagnetic iron using the electron spin resonance (ESR) method. These spectra and the magnetic data referenced above indicate up to ~4.5 wt% metallic iron in 60315.

Elastic wave velocities at pressures up to 10 kb were measured by Mizutani and Newbigging (1973) (Fig. 12). These data closely match the seismic velocity profiles from 5-25 km depth in the moon.

Chung and Westphal (1973) note the unusual electrical properties of 60315. The dielectric constant, dielectric losses and conductivity are all high (Figs. 13 and 14) possibly owing to the high concentration of metallic iron in the rock.

Charette and Adams (1977) provide visible and near-infrared reflectance data.

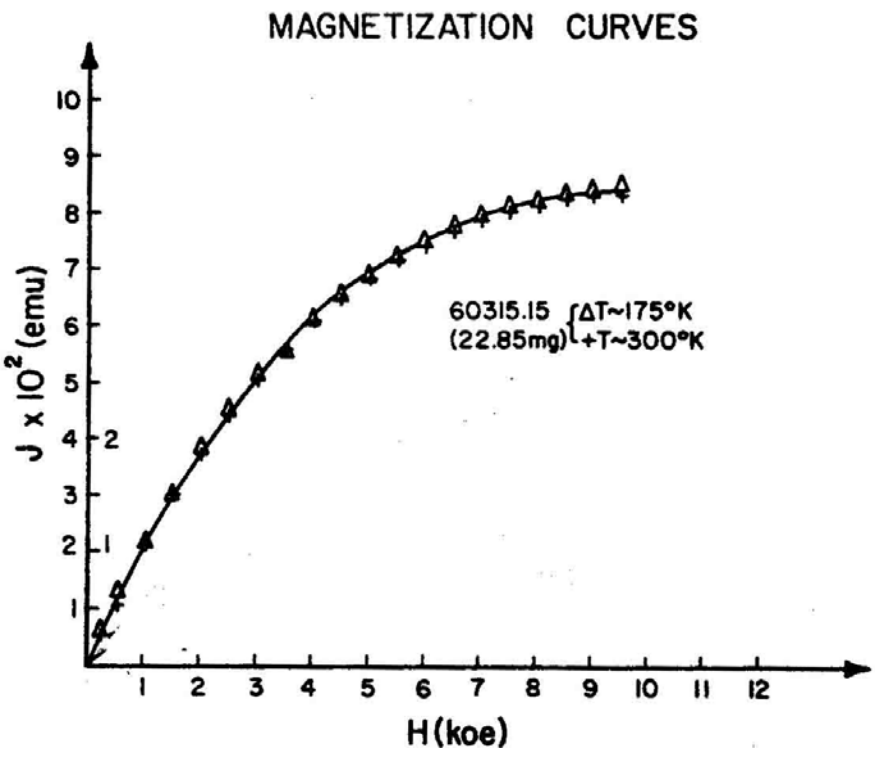


FIGURE 9. Magnetization; from Brecher et al.(1973).

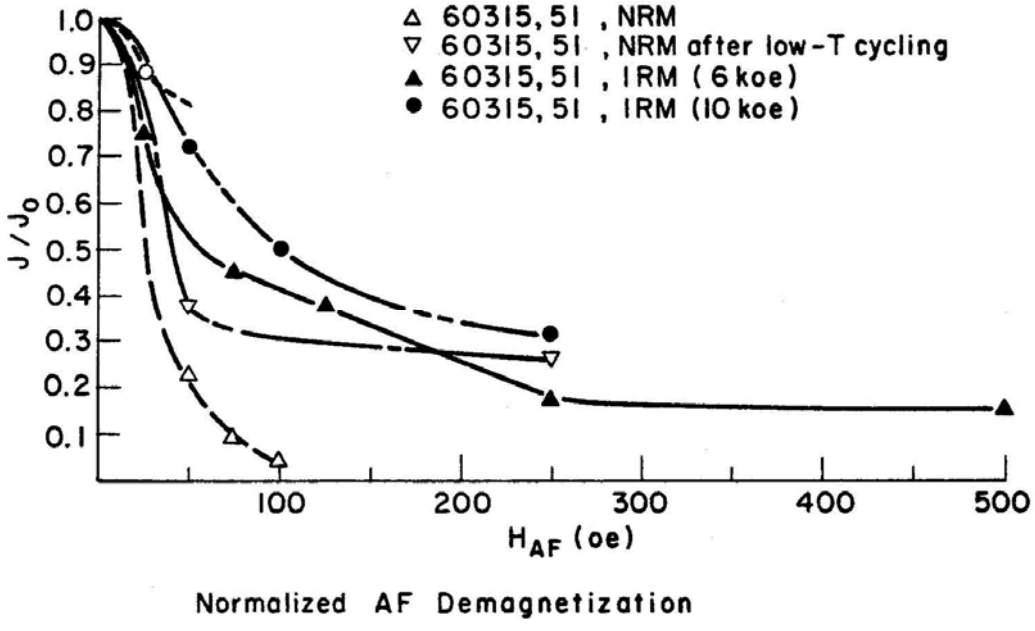


FIGURE 10. AF-demagnetization; from Brecher et al. (1973).

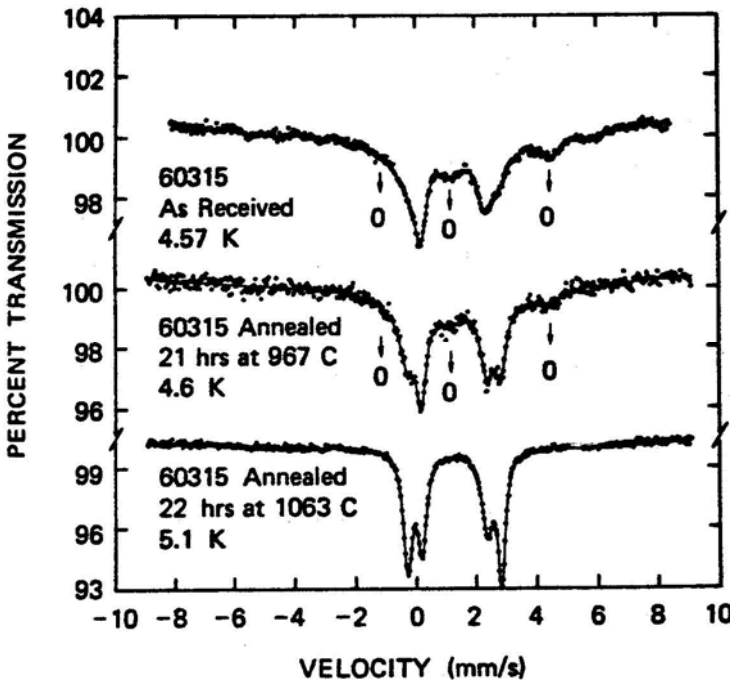


FIGURE 11. Liquid-helium spectra ;from Huffman and Dunmyre (1975).

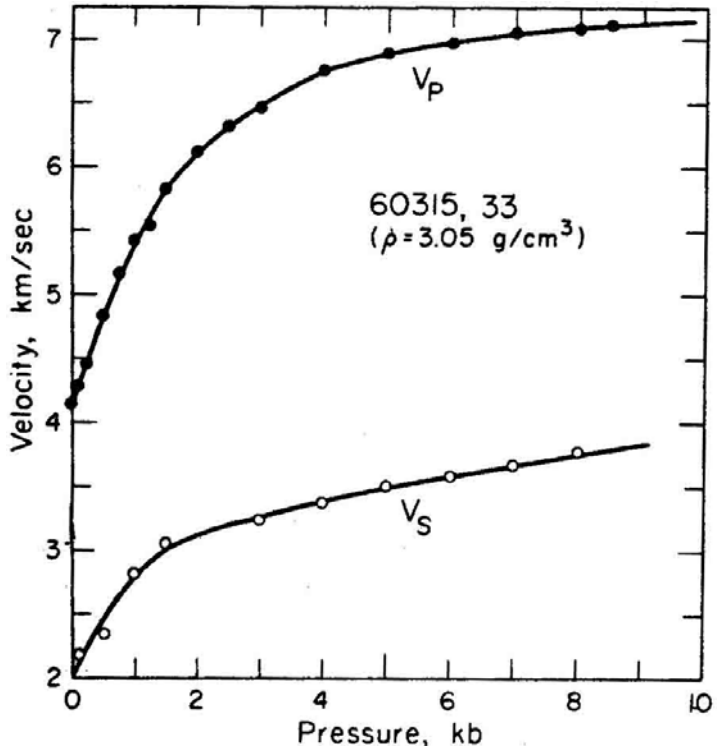


FIGURE 12. Elastic wave velocities; from Mizutani and Newbigging (1973).

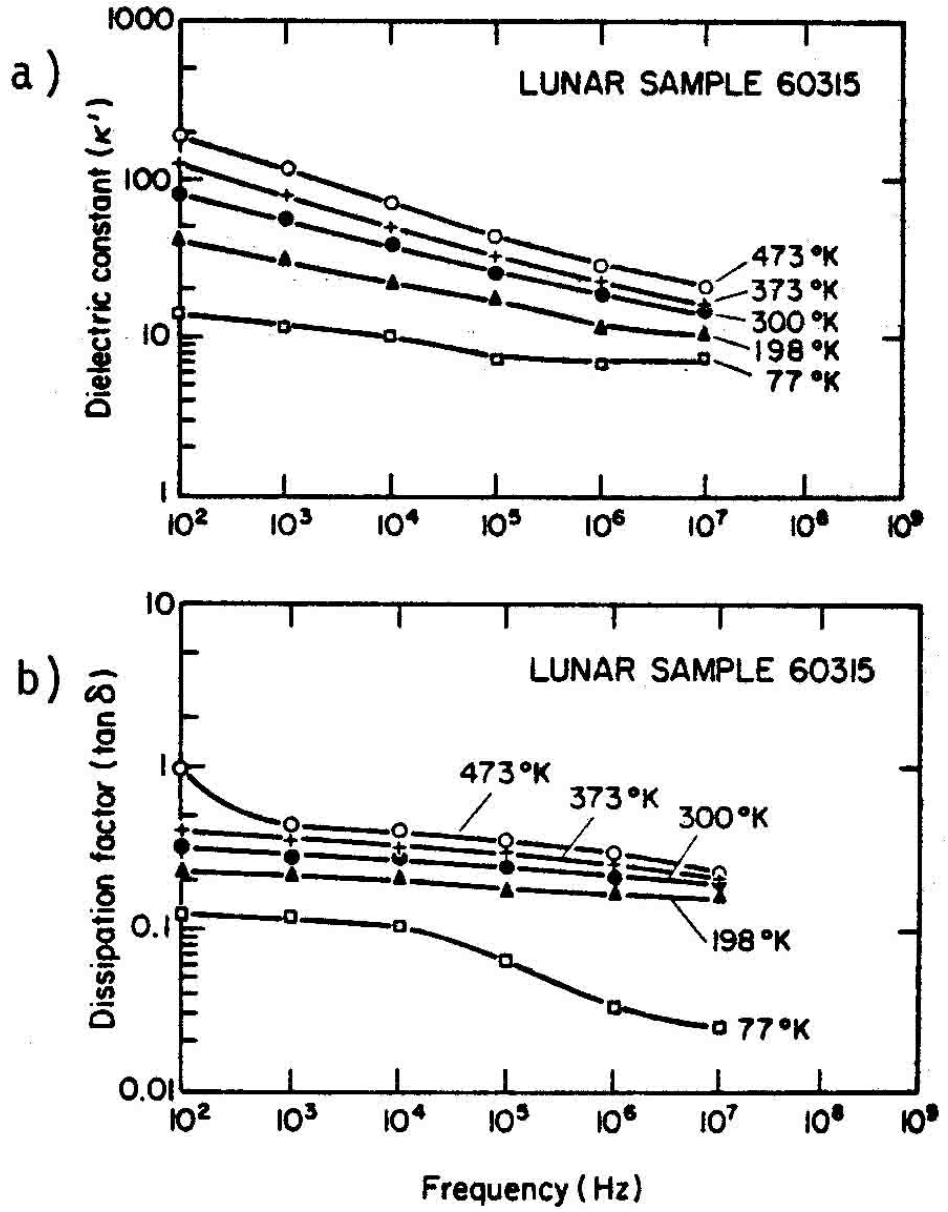


FIGURE 13. From Chung and Westphal (1973).
a) dielectric constant b) dielectric losses.

PROCESSING AND SUBDIVISIONS: This rock has been extensively subdivided and widely allocated. In 1972, it was cut into four pieces, including a slab (Figs. 15, 16). Allocations were primarily from the slab, from ,18 (entirely subdivided as ,47-,59 and ,79-,97) and from chips of ,0. The largest single piece remaining (,0 in Fig. 16) weighs 594.3 g and has been renumbered ,46. Serial thin sections were made from slab pieces ,20 and ,26. Thin sections also sample other portions of the rock. Many interior and exterior splits exist.

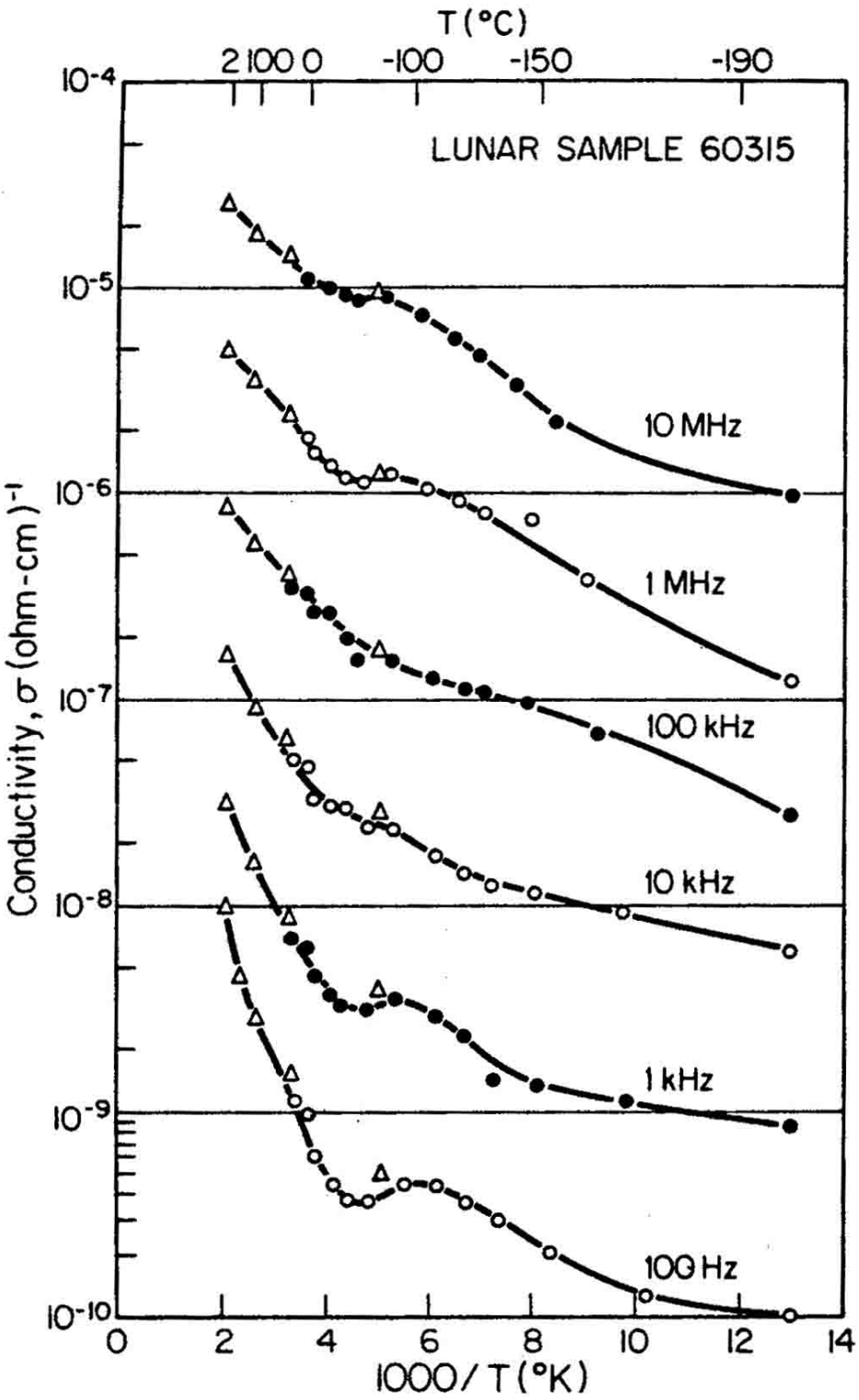


FIGURE 14. Electrical conductivity; from Chung and Westphal (1973).

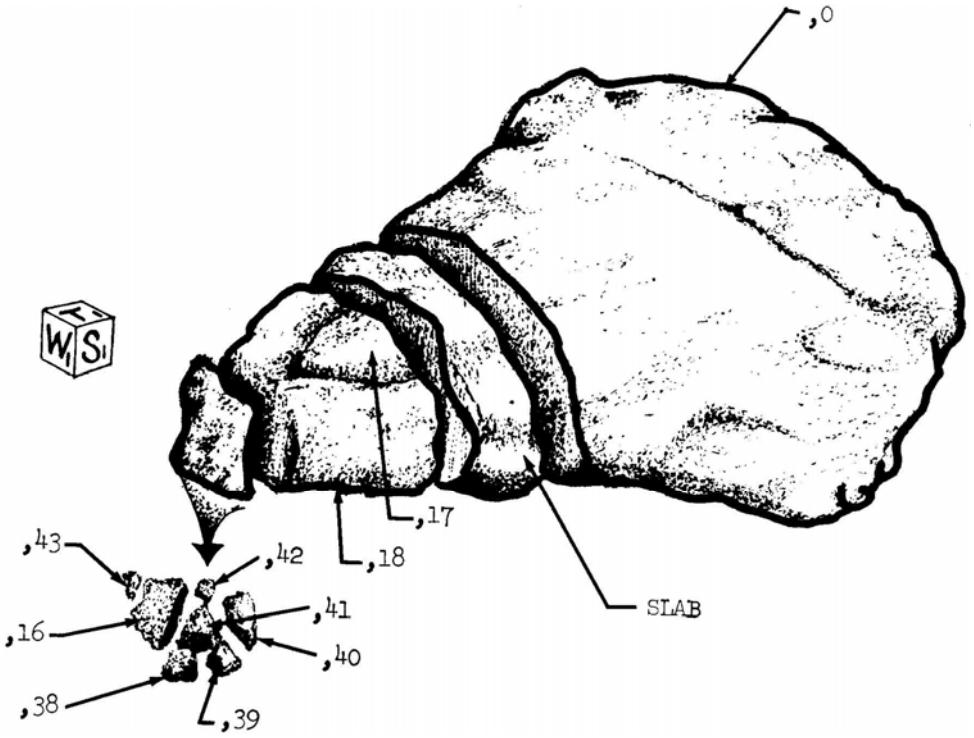


FIGURE 15. Cutting diagram.

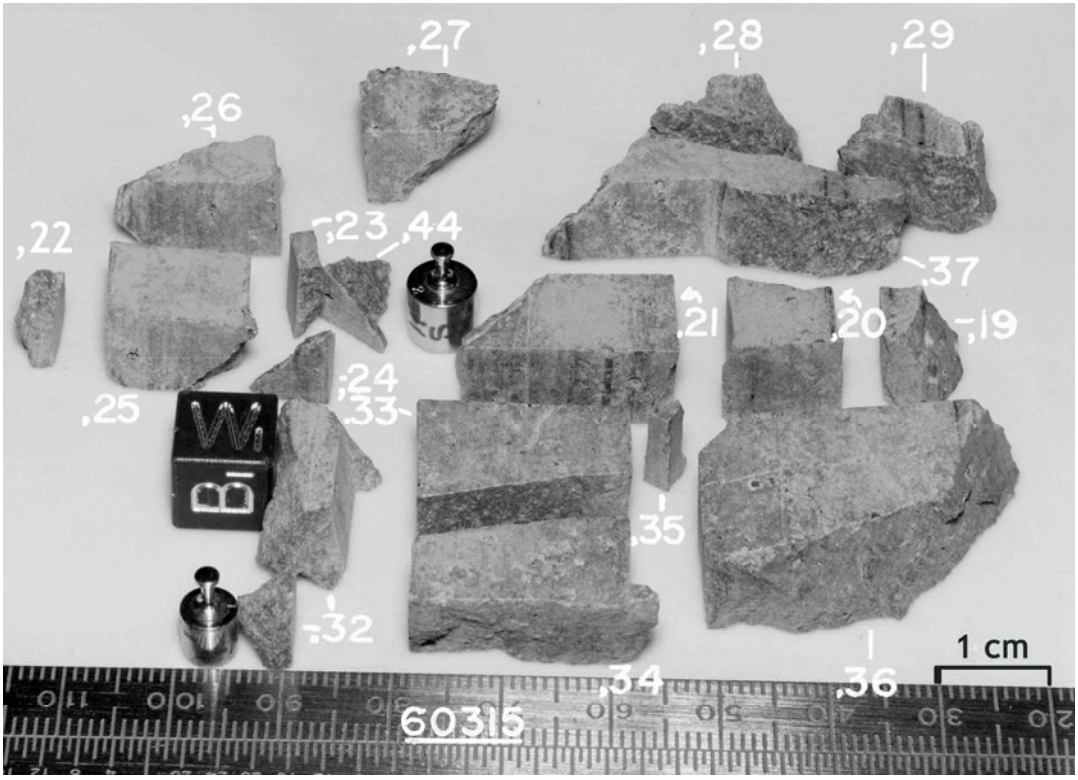


FIGURE 16. Main slab dissections of 60314. S-72-51842.